



UNIVERSITY OF LEEDS

This is a repository copy of *Gastric Cancer Screening in Low-Income Countries: System Design, Fabrication, and Analysis for an Ultralow-Cost Endoscopy Procedure*.

White Rose Research Online URL for this paper:
<http://eprints.whiterose.ac.uk/112610/>

Version: Accepted Version

Article:

Campisano, F, Gramuglia, F, Dawson, IR et al. (7 more authors) (2017) Gastric Cancer Screening in Low-Income Countries: System Design, Fabrication, and Analysis for an Ultralow-Cost Endoscopy Procedure. *IEEE Robotics & Automation Magazine*, 24 (2). pp. 73-81. ISSN 1070-9932

<https://doi.org/10.1109/MRA.2017.2673852>

© 2017 IEEE. Personal use of this material is permitted. Permission from IEEE must be obtained for all other users, including reprinting/ republishing this material for advertising or promotional purposes, creating new collective works for resale or redistribution to servers or lists, or reuse of any copyrighted components of this work in other works.

Reuse

Unless indicated otherwise, fulltext items are protected by copyright with all rights reserved. The copyright exception in section 29 of the Copyright, Designs and Patents Act 1988 allows the making of a single copy solely for the purpose of non-commercial research or private study within the limits of fair dealing. The publisher or other rights-holder may allow further reproduction and re-use of this version - refer to the White Rose Research Online record for this item. Where records identify the publisher as the copyright holder, users can verify any specific terms of use on the publisher's website.

Takedown

If you consider content in White Rose Research Online to be in breach of UK law, please notify us by emailing eprints@whiterose.ac.uk including the URL of the record and the reason for the withdrawal request.



eprints@whiterose.ac.uk
<https://eprints.whiterose.ac.uk/>

Ultra-low-cost endoscopy for gastric cancer screening in low-income countries

Federico Campisano¹, Francesco Gramuglia⁴, Imro R. Dawson³, Christopher T. Lyne¹, Michelle L. Izmaylov², Sarthak Misra^{3,6}, Elena De Momi⁴, Douglas R. Morgan², Keith L. Obstein^{2,1} and Pietro Valdastrì^{5,1}

¹STORM Lab USA, Dept. of Mechanical Engineering,
Vanderbilt University
Nashville, TN 37212, USA
federico.campisano.1@vanderbilt.edu, christopher.t.lyne@vanderbilt.edu

²Division of Gastroenterology, Hepatology and Nutrition,
Vanderbilt University Medical Center
Nashville, TN 37212, USA
michelle.l.izmaylov@vanderbilt.edu, douglas.morgan@vanderbilt.edu, keith.obstein@vanderbilt.edu

³Surgical Robotics Lab, Dept. of Biomechanical Engineering
University of Twente
Enschede, The Netherlands
i.r.dawson@student.utwente.nl, s.misra@utwente.nl

⁴Dept. of Electronics, Information and Bioengineering
Politecnico di Milano
Milano 20100, Italy
francesco.gramuglia@mail.polimi.it, elena.demomi@polimi.it

⁵STORM Lab UK, School of Electronic and Electrical Engineering
University of Leeds
Leeds, UK
P.Valdastrì@leeds.ac.uk

⁶Department of Biomedical Engineering
University Medical Center Groningen and University of Groningen
Groningen, The Netherlands
s.misra@umcg.nl

I. Introduction

Gastric adenocarcinoma is the fifth most common malignancy in the world and the third leading cause of cancer death in both women and men. In 2012, its estimated global incidence was of 952,000 new cases with an estimated 723,000 deaths worldwide [1, 2, 3]. It is projected to rise from fourteenth to eighth in all-cause mortality in the near term, primarily due to the growing and aging populations in the high incidence areas, such as Latin America and eastern Asia [4, 5]. Unlike any other major cancer, gastric cancer demonstrates marked geographic variability in regions and within countries, with more than 70% of incident cases concentrated in low- and middle-income countries (LMICs) [1,2].

Gastric adenocarcinoma is a multifactorial process, which progresses through a series of histopathology stages: normal mucosa, non-atrophic gastritis (NAG), multifocal chronic atrophic gastritis (CAG), intestinal metaplasia (IM), and finally to dysplasia and adenocarcinoma [6, 7]. The substrate leading to early gastric mucosal inflammation and chronic gastritis is driven by *H. pylori* infection, host genotypes and responses, and dietary and environmental factors [18]. Over 80% of the general population in LMICs of Central America (i.e., Honduras, El Salvador, Guatemala, and Nicaragua) are infected with *H. pylori* [6]. *H. pylori* eradication may help prevent gastric cancer in individuals with chronic gastritis, but is an inadequate strategy in patients with precancerous lesions. CAG, IM, and dysplasia are considered premalignant lesions, and are also highly prevalent (20-25%).

Early detection of premalignant lesions effectively reduced the mortality rate associated with gastric cancer in Japan and Korea [19]. Gastric cancer screening procedures are conducted at regional or urban medical centers using flexible endoscopes, which

provide high definition video and a tool channel for interacting with the tissue (e.g., tissue biopsy, endoscopic mucosal resection (EMR)). After a procedure, the flexible endoscope needs to be reprocessed in order to sanitize it for the following case [8].

Despite the high incidence of gastric cancer and the critical need for early detection, screening programs with flexible endoscopy are not common in LMICs and remote locations. The high initial cost of an endoscopic tower (e.g., about 80,000 USD), the cost and the time associated with repairing the instrument (flexible endoscope repairing centers are rarely located in LMICs), and the need for specialized equipment for reprocessing the endoscope in between procedures are the most relevant roadblocks to screening programs in LMICs. The limited portability of flexible endoscopes also limits screening to patients near regional or urban endoscopy centers.

An endoscopic platform for upper gastrointestinal (UGI) cancer screening programs in resource-limited and/or remote areas of LMICs would ideally need to be simple to control within the esophagus and stomach, easy to transport between remote locations, mechanically robust, disposable for sanitation, and ultra-low-cost (2-5 USD per procedure).

Alternative endoscopic screening technologies that could potentially be used in LMIC include capsule endoscopes and robotic endoscopy. Capsule endoscopes provide sanitary screening through disposability without the need for reprocessing [9], but they lack controllability and have a high cost-per-procedure (about 500 USD) [10]. Robotic endoscopy – still at the stage of preclinical [11], [12] or pilot clinical [13] trials – provides a highly controllable option, but also comes with a high cost-per-procedure that is not suitable for LMICs. Despite the considerable need for endoscopic screening technologies suited to low resource settings, there are currently no options that meet the unique needs of LMICs.

The HydroJet endoscopic platform was previously introduced in [14], showing potential for enabling screening programs in LMICs and rural or remote locations. The HydroJet (Fig. 1) is a soft-tethered endoscopic capsule that is maneuvered using three water jet actuators. In contrast to the Bowden cable actuation used in flexible endoscopes, jet actuation allows for a simple flexible tether that can be produced at a low cost. Our solution is intended as a pure diagnostic device (i.e., no therapeutic or instrument channel) with the intent of identifying suspicious lesions optically and then triaging patients to a regional or central urban endoscopy unit for traditional therapeutic endoscopy with biopsies/mucosal resection. With our technology, we are targeting a population that would otherwise not be screened and subject to high disease incidence and mortality due to the numerous barriers to standard flexible endoscopic screening in rural/remote areas of Central America.

Despite addressing the sanitation and cost needs of LMIC, the HydroJet design presented in [14] did not provide adequate controllability for a high-quality screening procedure. The jet actuation control was confined to three discrete settings (high, medium and low throttle), greatly limiting the resolution of motion control. In the previous system, water for jet actuation was pressurized by a diaphragm pump, which both relies on external power and has a wetted path that is not inert. Non-inert parts will corrode after long-term exposure to water, affecting system operation and potentially contaminating water used for the procedure and endangering patients.

Recently, the HydroJet has undergone further development and shows greatly improved controllability and portability, thus paving the way for translation to human trials. This paper presents the current platform and discusses the implications of the design optimization for the clinical efficacy of the device. Firstly, the number of actuating jets was reduced to three, enabling smaller capsule and tether diameters. The efficiency of the jet actuators was greatly improved, requiring less water per procedure.

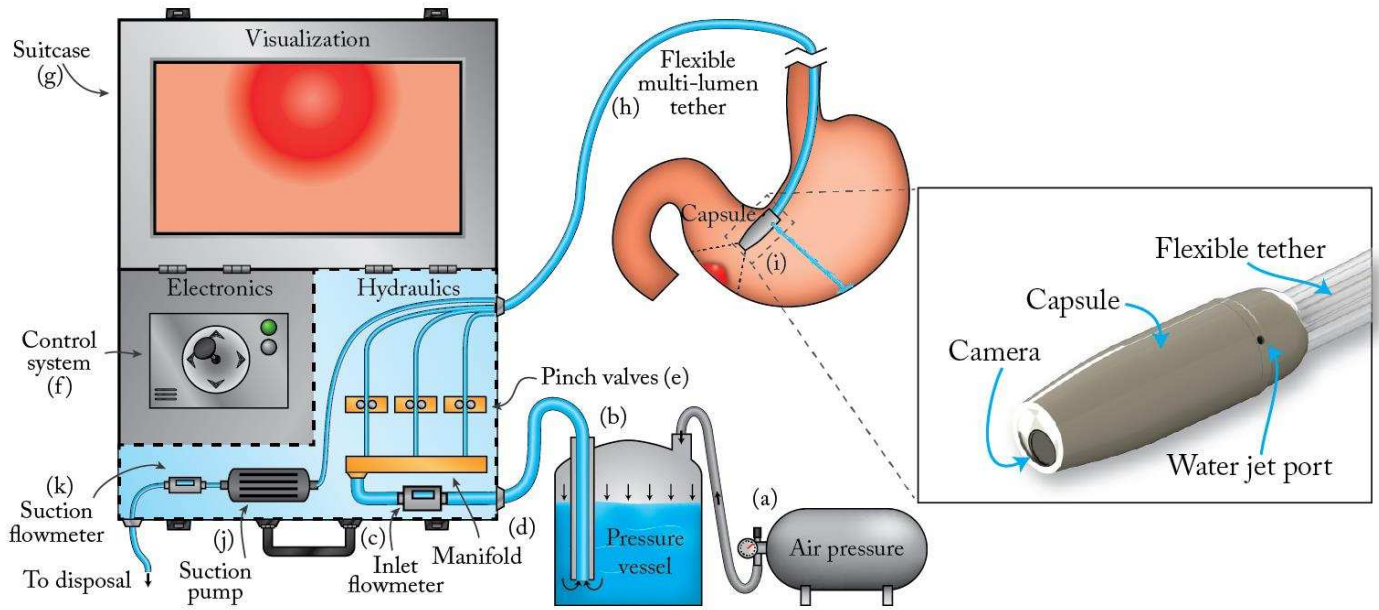


Fig. 1 Diagram of the HydroJet system: (a) Air pressure tank, (b) Dispensing pressure vessel, (c) Inlet flowmeter, (d) Manifold, (e) Pinch valves, (f) Control system, (g) Suitcase, (h) Multi-lumen tether, (i) Capsule, (j) Suction pump, (k) Suction flowmeter.

The water distribution system was changed substantially to provide an inert wetted path and independent, high-resolution control of the jet actuators. A single multi-lumen catheter was adopted instead of a bundle of single plastic tubes. Finally, the platform was redesigned to fit inside a suitcase the size of an airline carry-on, thus improving portability. The power consumption of the entire platform was optimized to be easily adapted to battery operation. These improvements make the HydroJet well suited as a screening aid to complement flexible endoscopes in LMIC.

II. Platform Overview

The HydroJet is an endoscopic platform (Fig. 1) designed for upper gastrointestinal cancer screening. The capsule (10 mm diameter by 29 mm length) carries a camera within a hermetically sealed shell (Fig. 2 (b)). The camera, which contains embedded light emitting diodes (LEDs) for illumination, is loaded into the back half of the capsule shell and connects through a four prong snap connector. The front half of the capsule is then attached to restrain the camera and seal the capsule. The capsule body contains three jet ports, spaced at 120° each around the diameter, which serve as actuators when pressurized water is ejected from the capsule. Jet actuation force is controlled externally by the components in the suitcase, resulting in a mechanically simple capsule design. The HydroJet is designed with disposable and reusable components (see Fig. 2 (c)). After completion of a cancer screening procedure, the HydroJet outer shell and tether are discarded and the capsule's camera (preserved from patient contact by the outer shell) is reclaimed without reprocessing.

The capsule and tether form a system that is similar to traditional endoscopes. Through selectively throttling each of the water jets, the HydroJet can autonomously pan the capsule with two degrees of freedom (DoF). Linear control of the capsule is accomplished by pushing/pulling the tether. Adjustment of the tether pivot length can be varied as needed to visualize the entire esophagus and stomach. By combining the 2 robotic DoFs, and a manual DoF given by pushing and pulling the tether, the HydroJet can achieve 3-DoF motion to explore the gastric cavity. Suction to remove the excess of water from the stomach is provided through the tether by a dedicated line, which does not require an additional port on the capsule.

The hydraulic system, part inside the suitcase, is designed to precisely regulate flow to each of the capsule jets, and in turn control jet actuation force. Compressed air is used to pressurize water in a dispensing pressure vessel (Fig. 1). The water is delivered from the vessel (b) to a distribution manifold (c). Throttle control of the jets is achieved using a set of proportional pinch valves (d), which independently regulate the flow rate of each jet. These valves use a specialized piston to pinch the line closed without contacting the water, and provide a simple and responsive way to control the flow. Suction is provided through the multi-channel tether into a hygienic receptacle. Similarly to traditional endoscopy, a button can be depressed at the endoscopist's discretion to trigger the pump and begin suction. In case of suction lumen obstruction, backflow flush—as in traditional endoscopy, can be performed to clean and clear the suction port. Two flowmeters (c and k in Fig. 1) monitor the rate of fluid flow to and from the stomach, in order to maintain a safe balance (typically around 1.3 liters).

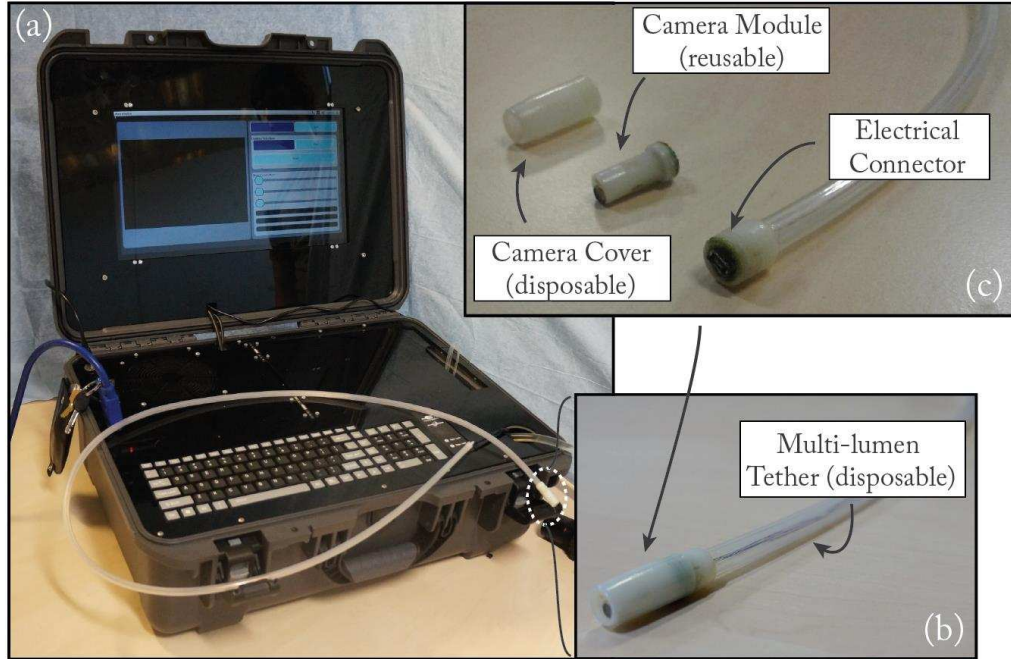


Fig. 2. (a) HydroJet platform designed to be easily transportable. (b) Picture of the HydroJet capsule. (c) The HydroJet capsule disassembled into disposable and reusable components.

III. System Design and Fabrication

A. Capsule

The capsule components are made from a durable plastic (Objet Verowhite Plus) via 3D printing (Objet Geometries Ltd., Model: OBJET 30). While this material is not medical grade, it is currently used due to its low price and availability. When moving forward with clinical trials, a biocompatible material such as polyether-ether-ketone (PEEK), will be used for capsule fabrication. Suction is provided by a dedicated port off-board the capsule, thus eliminating the need for additional suction ports on the capsule. The reusable inner core (Fig. 2 (c)) contains the camera module (Aidevision, Model: AD- 3915): an ultra-mini endoscopic camera (Diameter: 3.9 mm, Length: 14.5 mm, 54° field of view, 65 USD), which is used for diagnostics and control of the capsule, and two ultra-bright LEDs. The inner core is hermetically sealed within the outer shell, which snaps together to facilitate easy loading/unloading between procedures. A four-pole female connector, located on the rear of the inner core, provides electrical connectivity through the multi-channel tether. The inner core module is easily inserted or removed from the outer shell, allowing on-board electronics to be reclaimed and reused.

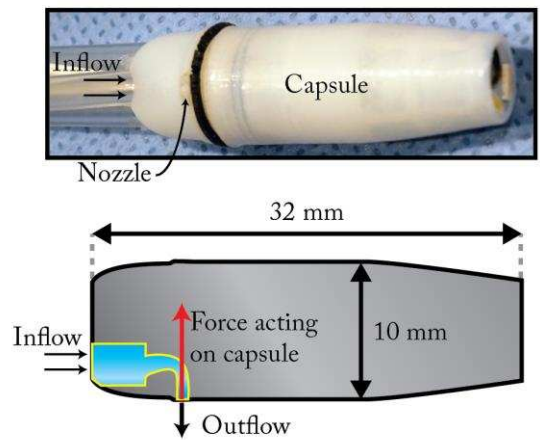


Fig. 3. Capsule cross-section. Three miniature nozzles are carved inside the capsule body with a spacing of 120° around the diameter.

The jet ports feature a converging nozzle design (Fig. 3 (b)), and jet actuation force is controlled by the hydraulic system. The purpose of the converging design is to accelerate the flowing water as it leaves the capsule, thus producing a reaction force in the opposite direction. The nozzle entrance is 1.6 mm to match the internal diameter of the jet tubes, and the nozzle exit diameter is 0.75 mm. The smooth transition between the inlet and outlet diameters contribute to an efficient nozzle design by eliminating regions of recirculating flow. The actuating force produced by this nozzle design was experimentally characterized, with a nozzle pressure drop of up to 3.85 bar, and was shown to give efficient propulsive performance throughout the operational range of the jet.

B. Multi-lumen tether

A custom-made multi-lumen tether connects the capsule to the water distribution system and is composed by seven total lumens, one centrally located and the remaining six divided equally around the diameter. The cross section is designed so that it incorporates channels for actuation, suction, and wiring. All outer channels are equally spaced and identical in shape and dimensions. Three of these channels are used for actuation and the other three are used for suction. Although it would be possible to have only a single channel available for suction, and thus having only four outer channels, this could cause undesirable bending behavior. By using six channels, the nozzles for the jets always line up with the channels supplying them with water. Additionally, with the current design the bending stiffness in each jet's bending direction is identical, which would not be the case with only four outer channels. The central channel is used for the wiring of the capsule. This way all wires are close to the neutral axis of the tether, limiting their effect on the bending stiffness of the total tether. Additionally, strains near the neutral axis are low during bending, reducing the chance of damage to the wires. In order to extrude the multi-lumen tether, a custom pin and die set was fabricated. The medical-grade silicone material, Nusil 4080, was used for the extrusion.

C. Suitcase

The platform was developed for easy transport and storage in a compact and durable suitcase that contains all of the components of the system (Fig. 1). The suitcase is divided into hydraulics, control electronics, and visualization sections. Each of the three sections was designed to be hermetically separated thus allowing for protection from potential water damage. In keeping with the design goals of the water distribution system, the pinch valves (Resolution Air, model: MPPV-2) provide flow control without exposing the valve parts to the water. This inert wetted path is an advantage in LMIC due to the lack of training and other resources necessary for routine maintenance. This design ensures that corrosion from exposure to potable water will not occur with long-term use, and that the water will not be contaminated prior to delivery to the patient. This makes the HydroJet platform inherently safe, as lack of proper maintenance or operation will not present any health complications to the patient.

The operator controls the HydroJet through a custom user interface implemented on an Arm A8-Cortex processor running Linux. The images streaming from the capsule's camera and the opening level for each of the pinch valves are shown on the monitor in real-time, together with the amount of water currently present in the patient's stomach, as measured by the flowmeters.

D. Dispensing Vessel and Air Tank

The dispensing pressure vessel (Millipore, Model: 6700P05, Volume: 5 Liters, Max operating pressure: 100 psi) is responsible for providing the pumping power for the jet actuators. The vessel contains enough water for approximately two screening endoscopies, and can be refilled without stopping the procedure. Compressed gas is used to pressurize the vessel, and water is expelled from the vessel through a dip tube (Fig. 1). The use of the dispensing pressure vessel greatly simplifies the pumping system so that only inert parts contact water, favoring long-term system reliability and patient safety. Alternative pump options such as peristaltic pumps are often used when an inert wetted path is needed, but despite this and resistance to occlusion, the output pressure and flow rate fluctuates drastically over a pumping cycle. These fluctuations result in an unsteady jet force and unstable capsule motion, interfering with visual diagnostics. In contrast, pneumatic pressurization does not rely on reciprocating parts, and can provide an inherently stable delivery pressure to enhance capsule stability. Another notable advantage of pneumatic pressurization is the independence from electrical power. Since compressed air can be carried in commercial tanks, this approach offers unique advantages in terms of portability and utility in LMIC.

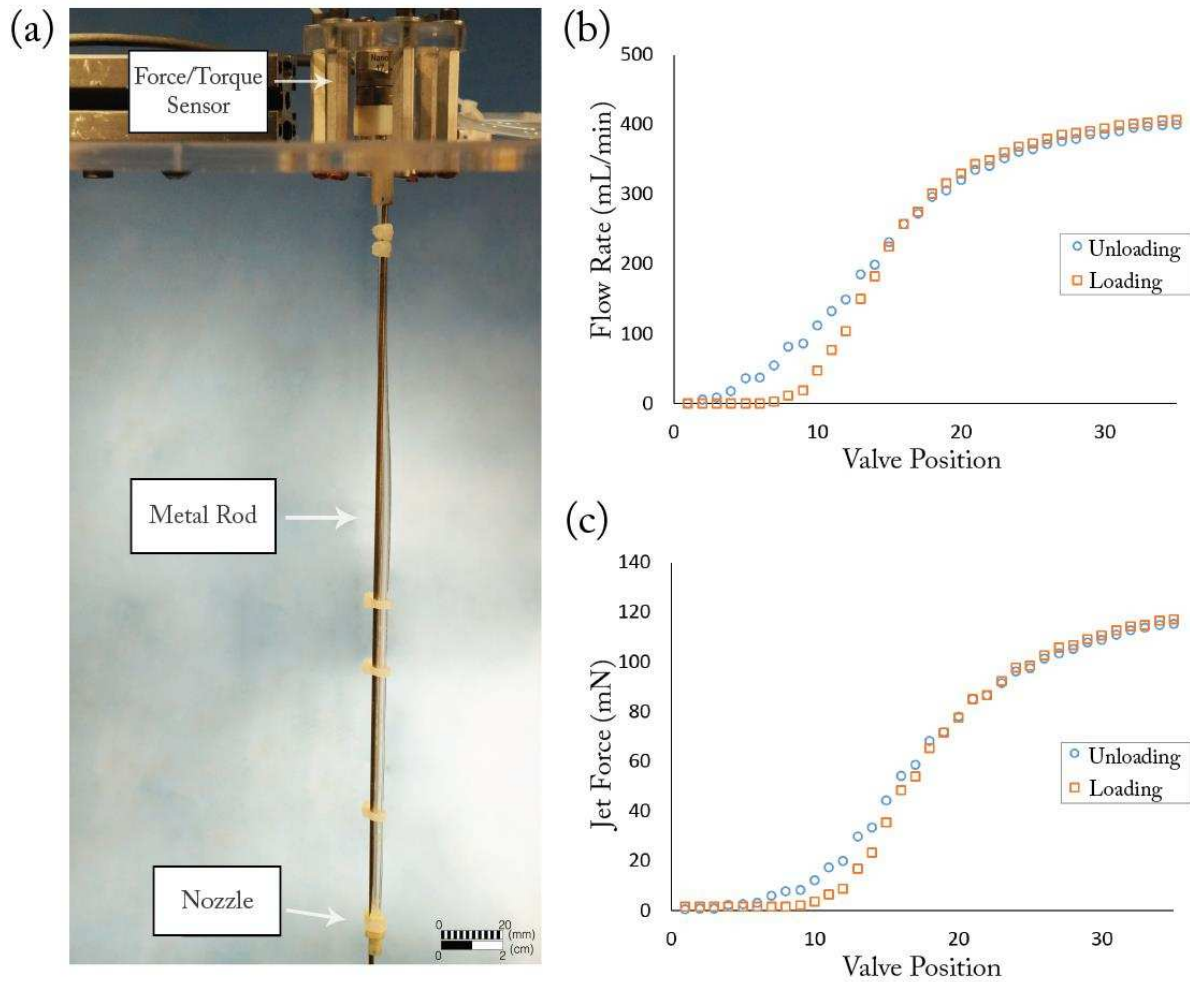


Fig. 4. (a) Experimental setup during the force characterization experiment. (b) Jet flow rate as a function of valve position. (c) Jet actuation force as a function of valve position.

IV. Experimental Analysis

1) Force Characterization

Characterization of water actuation force was performed to establish the relationship between valve position and jet force, and to examine hysteresis in jet control. Jet force was measured using a calibrated load cell (ATI Industrial Automation, Model: NANO17, resolution 0.318 gram-force). The capsule was connected to the load cell using a 265 mm rod and jet force was measured using a cantilever arrangement (Fig. 4 (a)). Five trials were conducted showing good repeatability of results. At a standard system pressure of 80 Psi, the maximum measured actuation force was 0.128 N with the valve fully opened. The measured jet force as a function of valve position (Fig. 4 (c)) exhibits a linear region in the center of the input range, which is favorable for capsule controllability.

Although control is repeatable, hysteresis is present between the opening (unloading) and closing (loading) of the valve. This discrepancy is likely due to positional inaccuracies in the pinch valves themselves, rather than a fluid dynamical hysteresis.

2) Flow Rate Characterization

Jet flow rate was measured during jet force testing using an ultrasonic flowmeter (Atrato, Model: Titan 760), which provides the instantaneous flow rate through the jets. Basic fluid dynamics theory dictates that for a non-deforming system at steady state, jet force is a function of flow rate alone. This relationship provides a basis for control of the jet actuation force.

As expected from the jet force measurements, hysteresis in flow control is present in the experimental data (Fig. 4 (b)). Although fluid flow should show no hysteresis, pinch valves rely on a mechanical drivetrain and show some error in control. The hysteresis is seen to increase as the valve clamping force increases, due to the greater forces imposed on the valve drivetrain. When loaded, both frictional forces and motor dynamics contribute to hysteresis in the drivetrain. Using a fixed upstream pressure of 80 Psi, the maximum measured flow rate was 410 mL/min that agrees with classical fluid modeling equations.

3) Range of Motion using a Single Jet

This experimental trial aimed at understanding the controllability of the capsule while throttling a single jet from fully closed to fully open. Camera stability for internal visualization is the main requirement for any endoscopic platform. This trial was carried on to quantify the number of stable positions the capsule can reach and the maximum displacement that can be obtained with respect to the free length of the tether. To be considered a stable position, the capsule must be still enough to use the camera for visual inspection. The capsule motion was monitored using a 6-DoF magnetic coil (0.9 mm diameter, 12 mm length) embedded in the capsule and excited with an electromagnetic transmitter (Northern Digital Inc. (NDI), Model: AA138). During the study, the tether was secured and held vertical using an aluminum metallic arm with a custom 3D printed holder to provide a well-defined pivot point (Fig. 5 (a)). Water was fed to the capsule internal nozzles using the multi-lumen catheter described in section B.2. Three different tether length (L) 6 cm, 9 cm, and 12 cm were tested in order to obtain the relationship between lateral and vertical displacement and therefore quantify the maximum motion with respect to the vertical position (Fig. 5 (a)). A single sweep motion (Fig. 5 (b)) was programmed using the suitcase control electronics. The sweep consisted of gradually controlling the jet pinch valve, sending the capsule one step forward command every 5 s, until the valve was completely open.

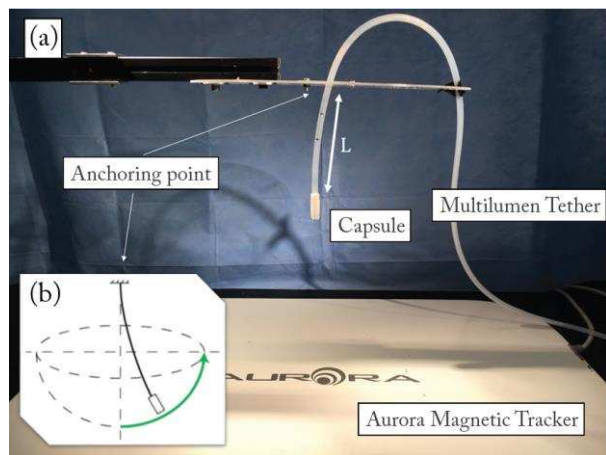


Fig. 5. (a) Custom experimental test-bench: The capsule was held vertically using an aluminum metallic arm with a custom 3D printed holder to provide a well-defined pivot point. (b) Programmed sweep operated controlling only one pinch valve sending one-step forward command every 5 s until the valve resulted completely open.

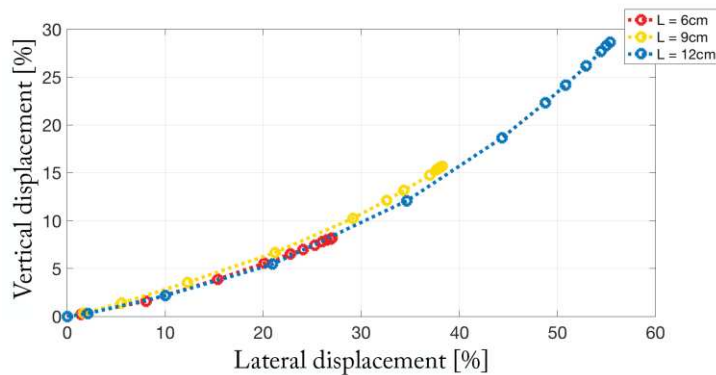


Fig. 6. Single jet motion result: A total number of 13 stable points (dots) were found after the trial for each tether length. Maximum lateral displacement of 56% with respect to the tether length corresponds to 6.60 mm or 50° angle with respect to the vertical.

A plot of the stable positions reached by the capsule is shown in Fig. 6. Thirteen stable position were found for each tether length that correspond to 2197 positions using the combination of three jets. The experiment shows repeatability of the results despite varying the tether length. The motion was constrained, as expected, in a semi-hemispherical workspace. The maximum lateral displacement was 56%, 38% and 28% of the 12 mm, 9 mm and 6 mm free lengths, respectively. These results show maximum angle of 50° from the vertical that can be adjusted changing the tether length without losing controllability. This is the most important result since controllability is guaranteed even with changes in the anchoring point, and means that many common tasks, such as retroflexion, can be obtained by pushing more tether inside the stomach while adjusting the position using jet propulsion.

4) Full Workspace Characterization

To obtain the full hemispherical capsule workspace (Fig. 8 (a)(b)), multiple jets must be actuated at once. The full workspace was explored using the custom test-bench of Fig. 5 (a) and the system was programmed to follow the path shown in Fig 7 (a). The path consisted of the following steps: (1) starting from the free vertical position, one jet was throttled up until the full power was reached, then the capsule starts travelling around in a circle using combination of jets. The path continued by throttling up the second jet until the maximum power was reached while the first one was still active (2). Then, the first jet was decreased gradually to zero

(3) and the same pattern was followed with the remaining jet until the capsule returned to the initial position (4). For better understanding of the reader, actual pictures of the HydroJet following the programmed path are shown in Fig. 7 (b).

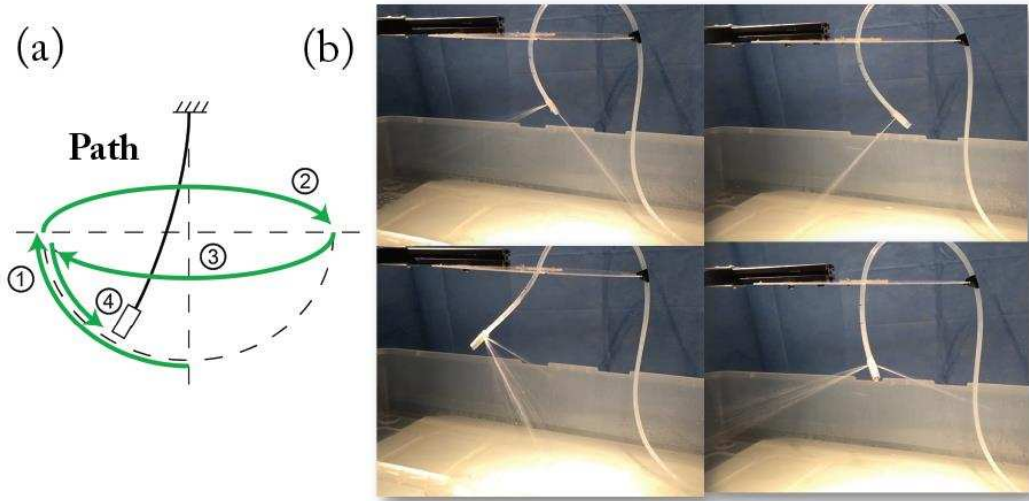


Fig. 7. (a) Programmed path. (b) Pictures of the HydroJet capsule travelling around the programmed path to characterize the full workspace.

By controlling the actuation force of each jet individually, the jets can produce a resultant motion in 2-DoF. As in the previous trial, three different tether lengths were tested, 12 cm, 9 cm and 6 cm, and each one was restrained from rotating. The resulting capsule motion demonstrated maneuverability in a quasi-hemispherical workspace (Fig. 8 (a)). A bidimensional side view of the capsule workspace is given in Fig. 8 (b). There are six peaks in Fig. 8 that correspond to the characteristic travelling motion of the HydroJet. They are due to the geometric location of the nozzles on the capsule. Once a second jet couples with an active jet, the capsule is pushed down and recovers the original height only when the two jets provide an equivalent reaction thrust. The workspace shows repeatability and symmetry with respect to change in tether length. In addition, the capsule was able to return to the initial position after traveling along the path. The maximum lateral displacement recorded for the 12 cm tether was around 6 cm, corresponding to an equivalent hemispheric diameter of 12 cm, the same length as the tether.

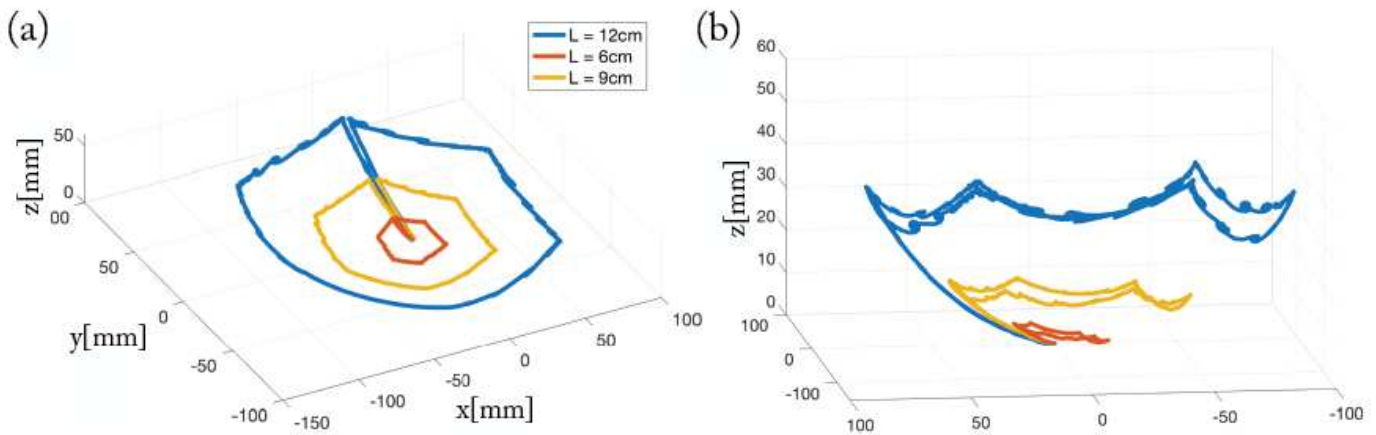


Fig. 8. (a) Full semi-hemispherical workspace using different tether length (L) (Top View). (b) Full semi-hemispherical workspace using different tether length (L) (Lateral View).

5) Stomach Phantom Retroflexion Trial

To validate the feasibility of retroflexing the capsule within a confined space, an anatomically realistic human stomach phantom was used for this trial. The phantom, having the size of an average adult stomach (internal volume ~ 1000 cm³ [20]), was fabricated at Vanderbilt University Medical Center using a 3D mold from a human stomach CT scan reconstruction and a mixture of silicone rubbers (Dragonskin30 and Ecoflex10: 1-2 ratio, Smooth-On, USA) to match the original tissue properties. As briefly introduced before, retroflexion can be performed by advancing the tether further into the stomach while using the opposite wall of the cavity to deflect the movement (similar to the mechanics of retroflexion when using a traditional endoscope). The different phases of the procedure can be seen in Fig. 9. As illustrated, the capsule is initially directed toward the greater curvature wall by throttling one jet (a). The operator, maintaining the same throttle, pushes the tether until the capsule hits the stomach wall (b). By looking at the image from the camera, the operator now uses the wall to pivot the capsule by controlling the amount of tether inserted (c). Once the capsule is lying against the wall, water jets are again used to complete retroflexion (d).

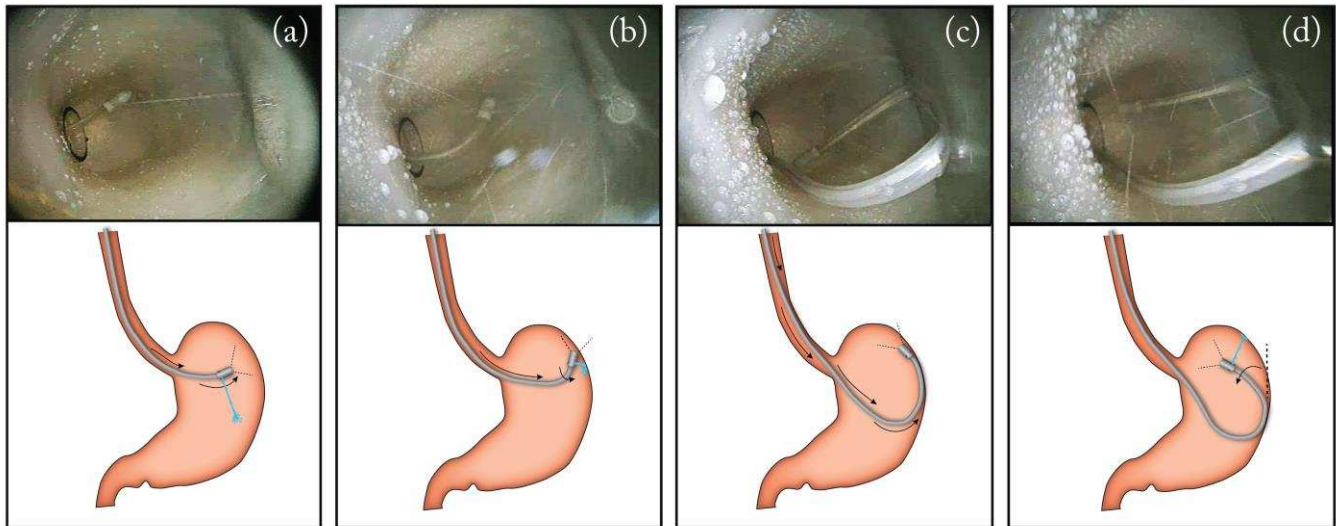
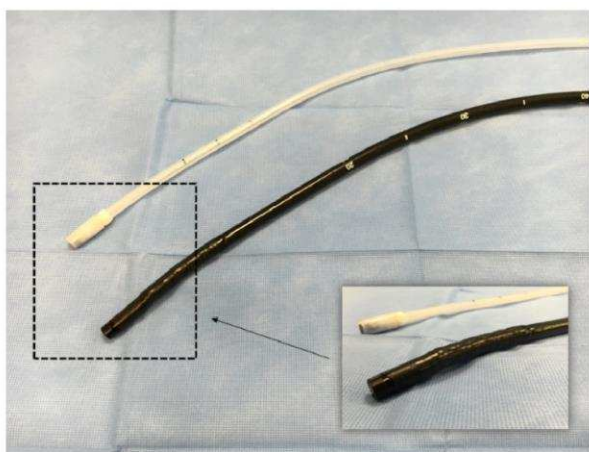


Fig. 9. Different phases of a retroflexion maneuver.

During this set of trials, an expert endoscopist (attending physician who has performed more than 2,000 lifetime endoscopies) attempted retroflexion ten times with both the HydroJet and with a standard upper endoscope (Karl Storz, Tuttlingen, Germany). All trials were successful. The average time to perform the maneuver was 32 seconds with the HydroJet and 5 seconds with the flexible endoscope.

6) Comparative Trial

A bench top trial was performed to compare the controllability of the HydroJet with a traditional flexible endoscope (Storz, Model: Pediatric Gastroscope), shown side by side in Fig. 10. A small opaque bucket was used to simulate the workspace of the stomach, and 3 sets of 6 points were marked on the inner wall for visual identification. The sets were differentiated by using a shape designator, either a circle, star, or square. Trials were then conducted with 4 novice users and 1 expert user (attending with more than 1,000 lifetime endoscopies), in which each user identified and navigated to each point within the set of points. Each user conducted three trials with the gastroscope and three trials with the HydroJet, and the total time of the procedure and time between points were recorded. The sets of points and endoscopic device for each trial were chosen in a randomized order to prevent memory bias from affecting the results. The results of this trial are reported in Fig. 10 for both expert and novice users.



| <i>Novice</i> | Endoscope | HydroJet |
|--------------------|------------------|-----------------|
| Total Time | 5:42 | 8:24 |
| Average Time | 0:19 | 0:28 |
| Standard Deviation | 0:13 | 0:25 |
| <i>Expert</i> | | |
| Total Time | 2:54 | 13:18 |
| Average Time | 0:10 | 0:44 |
| Standard Deviation | 0:06 | 1:11 |

Fig. 10. Results of comparative trials between the HydroJet and a standard flexible endoscope. Total time refers to the cumulative time to complete all three trials with a given endoscopic device, while average time and standard deviation refer to the time needed to identify a single point. Time data given in minutes:seconds format.

With novice users, the HydroJet took approximately 50% longer than the flexible endoscope to complete a procedure. With the expert user, the difference between the HydroJet and flexible endoscope was much larger due to the user's expertise in using traditional endoscopes. Although the HydroJet takes longer than the flexible endoscope to complete a screening procedure, it still can provide screening care in a reasonable amount of time, and shows potential for improvement with operator training.

It is worth comparing the optical capabilities of the HydroJet to that of the flexible endoscope to better understand the results. The endoscope used for comparison has a 140° field of view, and a focal distance of 2 mm-100 mm. In contrast, the camera used in the HydroJet has a 54° field of view and a focal distance of 10 mm - 50 mm. As such, the discrepancy in the quality of camera used in each device is expected to give the endoscope a baseline advantage, regardless of capsule controllability. Thus, these results can be considered to be a conservative estimate of the capabilities of the HydroJet. Of course, using a camera with a wider field of view would definitely reduce the time required to complete a procedure.

V. Conclusion and Future Work

The HydroJet endoscopic platform addresses the need for a low cost, portable system for upper gastrointestinal cancer screening in LMIC. In this study, a novel water distribution system is introduced, which addresses many of the deficiencies of the previous design. Open-loop and throttle control of the actuating jets are examined and show good controllability of the reaction thrust. The range of stable positions the capsule can reach was further examined and a total number of 2197 total positions were found for the three jets. This number is invariant on the tether length, depending only on the resolution of the pinch valve, which thus allows full controllability and stable spatial resolution with differing tether lengths. Finally, comparative trials were conducted to evaluate the medical practicality of the platform.

Future work includes the implementation of closed-loop control of jet actuation force, which can reduce the training required to operate the platform. This type of control could enable semi-autonomous operation, wherein the platform can help the user control movement of the capsule in order to visualize regions of interest. Even if retroflexion is feasible, the increased time required and the need to learn a new maneuver to reach adequate performance are limitations of the current platform that will be addressed in future work. Further demonstration of the capsule mobility both ex vivo and in vivo is needed to better assess clinical efficacy. Additional in vivo trials to assess the medical accuracy of the platform are planned, with the goal of a comparative assessment between the HydroJet platform and traditional endoscopy. With the success of medical trials, the HydroJet platform can address a deficiency in point-of-care medicine for the LMIC setting. More broadly, the HydroJet can enable the widespread implementation of UGI cancer screening programs, thus reducing the rate of incident cancers and global cancer mortality.

Acknowledgment

Research reported in this publication was supported by the NIBIB of the NIH under award number R01EB018992, by the NSF under grant number IIS-1453129 and CNS-1239355, by the Royal Society under grant number CH160052, by the EPSRC, by the ERC under grant agreement #638428, and by the Vanderbilt Institute for Surgery and Engineering (VISE). Any opinions, findings and conclusions or recommendations expressed in this material are those of the authors and do not necessarily reflect the views of the NIH, the NSF, the Royal Society, the EPSRC, the ERC, or VISE.

References

1. J. Ferlay, I. Soerjomataram, R. Dikshit, S. Eser, C. Mathers, M. Rebelo, D.M Parkin, D. Forman, F. Bray. Cancer incidence and mortality worldwide: sources, methods and major patterns in GLOBOCAN 2012. *Int J Cancer*. Mar. 2015.
2. J. Ferlay, H.R. Shin, F. Bray, D. Forman, C. Mathers, D.M. Parkin. Estimates of worldwide burden of cancer in 2008: GLOBOCAN 2008. *Int J Cancer*. 2010 Dec 15.
3. C. De Martel, J. Ferlay, S. Franceschi, J. Vignat, F. Bray, D. Forman, M. Plummer. Global burden of cancers attributable to infections in 2008: a review and synthetic analysis. *Lancet Oncol*. Jun 2012.
4. C. J. Murray, A. D. Lopez. Alternative projections of mortality and disability by cause 1990-2020: Global Burden of Disease Study. *Lancet*. May 1997.
5. P. E. Goss, et al. Planning cancer control in Latin America and the Caribbean. *Lancet Oncol*. Apr 2013.
6. D. B. Polk, R. M. Peek, Jr. *Helicobacter pylori*: gastric cancer and beyond. *Nat Rev Cancer*. Jun 2010.
7. P. Corre. *Helicobacter pylori* and gastric cancer: state of the art. *Cancer Epidemiol Biomarkers Prev*. Jun 1996.
8. K. J. Lee, M. Inoue, T. Otani, M. Iwasaki, S. Sasazuki, and S. Tsugane. "Gastric cancer screening and subsequent risk of gastric cancer: a large-scale population-based cohort study, with a 13-year follow-up in Japan," *Int. J. Cancer*, vol. 118, no. 9, pp. 2315–21, May 2006.
9. H. Makuuchi, T. Machimura, H. Shimada, K. Mizutani, O. Chino, Y. Kise, T. Nishi, H. Tanaka, T. Mitomi, M. Horiuchi, M. Sakai, J. Gotoh, J. Sasaki, and Y. Osamura, "Endoscopic screening for esophageal cancer in 788 patients with head and neck cancers," *The Tokai Journal of Experimental and Clinical Medicine*, vol. 21, pp. 139–145, 1996.
10. A. Oshima, N. Hirata, T. Ubukata, K. Umeda, and I. Fujimoto, "Evaluation of a mass screening program for stomach cancer with a case-control study design," *Int. J. Cancer*, vol. 38, no. 6, pp. 829–33, Dec. 1986.
11. T. J. Wilhelm, H. Mothes, D. Chiwewe, B. Mwatibu, and G. Ka'bler, "Gastrointestinal endoscopy in a low budget context: delegating EGD to non-physician clinicians in Malawi can be feasible and safe." *Endoscopy*, vol. 44, no. 2, pp. 174–6, Feb. 2012.
12. A. Koulaouzidis and S. Douglas, "Capsule endoscopy in clinical practice: concise up-to-date overview." *Clinical and Experimental Gastroenterology*, vol. 2, pp. 111–6, Jan. 2009.
13. D. S. Mishkin, R. Chuttani, J. Croffie, J. Disario, J. Liu, R. Shah, L. Somogyi, W. Tierney, L. M. W. K. Song, and B. T. Petersen, "ASGE technology status evaluation report: wireless capsule endoscopy." *Gastrointestinal Endoscopy*, vol. 63, no. 4, pp. 539–45, Apr. 2006.
14. S. Yim and M. Sitti, "Design and analysis of a magnetically actuated and compliant capsule endoscopic robot," 2011 IEEE Int. Conf. Robot. Autom., pp. 4810–4815, May 2011.
15. I. De Falco, G. Tortora, P. Dario, and A. Menciassi, "An integrated system for wireless capsule endoscopy in a liquid-distended stomach," *IEEE Trans. Biomed. Eng.*, vol. 61, no. 3, pp. 794–804, Mar. 2013.
16. J. F. Rey, H. Ogata, N. Hosoe, K. Ohtsuka, N. Ogata, K. Ikeda, H. Aihara, I. Pangtay, T. Hibi, S. Kudo, and H. Tajiri, "Feasibility of stomach exploration with a guided capsule endoscope," *Endoscopy*, vol. 42, no. 7, pp. 541–5, Jul. 2010.
17. R. Caprara, K. L. Obstein, G. Scozzarro, C. Di Natali, M. Beccani, D. Morgan, and P. Valdastrì, "A platform for gastric cancer screening in low- and middle-income countries," *IEEE Trans. Biomed. Eng.*, vol. 62, no. 5, pp. 1324 – 1332, 2015.
18. L. E. Wroblewski, R. M. Peek Jr, K. T. Wilson. *Helicobacter pylori* and gastric cancer: factors that modulate disease risk. *Clin Microbiol Rev*. Oct 2010.
19. K. J. Lee, M. Inoue, T. Otani, M. Iwasaki, S. Sasazuki, S. Tsugane. JPHC Study Group. Gastric cancer screening and subsequent risk of gastric cancer: a large-scale population-based cohort study, with a 13-year follow-up in Japan. *Int J Cancer*. May 2006.
20. Miyashita, Shuhei, et al. "Ingestible, controllable, and degradable origami robot for patching stomach wounds." *Robotics and Automation (ICRA)*, 2016 IEEE International Conference on. IEEE, 2016.